
Supporting Information

Multidimensional luminescent cobalt(II)-coordination polymers as sensors with extremely high sensitivity and selectivity for detecting of acetylacetone, benzaldehyde and $\text{Cr}_2\text{O}_7^{2-}$

Ai-Ling Li^a, Yun-Hua Qu^a, Lianshe Fu^b, Chao Han^a, Guang-Hua Cui^{a*}

^a*College of Chemical Engineering, Hebei Key Laboratory for Environment Photocatalytic and Electrocatalytic Materials, North China University of Science and Technology, No. 21 Bohai Road, Caofeidian new-city, Tangshan, Hebei, 063210, P. R. China*

^b*Department of Physics and CICECO-Aveiro Institute of Materials, University of Aveiro, 3810-193 Aveiro, Portugal*

* Corresponding author. Fax: +86-315-8805462, Tel: +86-315-8805460.

*E-mail: tscghua@126.com

Supporting Information

Content	Page (#)
1. Fig. S1. Each L ligand to link adjacent Co(II) centers into a 2D (4,4) layer of 1 .	3
2. Fig. S2. 1D wave-like [Co–TBTA–Co] _n chain of 2 .	4
3. Fig. S3. Uninodal hcb topology of 2 .	5
4. Fig. S4. SEM images of the powdered 1 , 2 and 3 .	6
5. Fig. S5. Different N-containing ligands connect adjacent Co ^{II} centers of 1 , 2 and 3 .	7
6. Fig. S6. Powder X-ray diffraction (PXRD) patterns of 1 , 2 and 3 .	8
7. Fig. S7. TGA curves of 1 , 2 and 3 .	9
8. Fig. S8. Time resolved luminescence decay curves of 1 , 2 and 3 .	10
9. Fig. S9. (a) Comparison of the luminescence emission intensity of 1 for sensing of acac/BZH in the presence of other organic solvents; (b) Comparison of the luminescence emission intensity of 2 for sensing of acac/BZH in the presence of other organic solvents; (c) Comparison of the luminescence emission intensity of 3 for sensing of acac/BZH in the presence of other organic solvents.	11
10. Fig. S10. (a) Stern–Volmer plot of $I_0/I - 1$ versus acac/BZH in different concentrations for 2 ; (b) Stern–Volmer plot of $I_0/I - 1$ versus acac/BZH in different concentrations for 3 .	14
11. Fig. S11. PXRD patterns of 1 , 2 and 3 after treating in acidic aqueous solution (pH = 3).	15
12. Fig. S12. Stern–Volmer plot of $I_0/I - 1$ versus Cr ₂ O ₇ ²⁻ ions in range from 0 to 2×10 ⁻⁴ M (top); Nonlinear Stern–Volmer of 1 , 2 and 3 in aqueous solutions with different concentrations (bottom).	16
13. Fig. S13. Luminescence emission spectra of CPs in water from 0 to 60 min by 5 min step.	17
14. Fig. S14. (a) PXRD patterns of the simulated of 1 after sensing of acac, BZH and Cr ₂ O ₇ ²⁻ for three cycles in water; (b) PXRD patterns of the simulated of 2 after sensing of acac, BZH and	

$\text{Cr}_2\text{O}_7^{2-}$ for three cycles in water; (c) PXRD patterns of the simulated of **3** after sensing of acac, BZH and $\text{Cr}_2\text{O}_7^{2-}$ for three cycles in water; (d) Comparison of the quenching efficiency of **1**, **2** and **3** for sensing of acac, BZH and $\text{Cr}_2\text{O}_7^{2-}$ over three cycles.

18

15. **Fig. S15.** (a) PXRD patterns of CPs and sensing for acac, respectively; (b) PXRD patterns of CPs and sensing for BZH, respectively; (c) PXRD patterns of CPs and sensing for $\text{Cr}_2\text{O}_7^{2-}$, respectively. 22

16. **Fig. S16.** (a) Spectral overlap between the absorption spectra of different solvents and the excitation spectra of **1**, **2** and **3**; (b) Spectral overlap between the absorption spectra of anions and the excitation spectra of **1**, **2** and **3**. 25

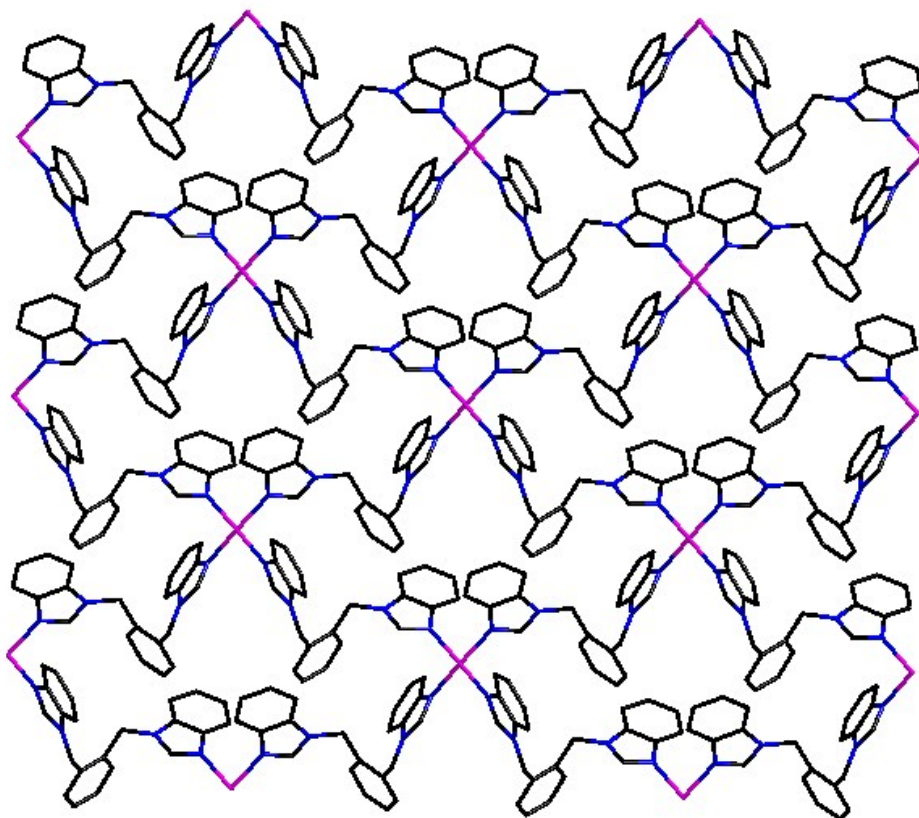


Fig. S1. Each L ligand to link adjacent Co^{II} centers into a 2D (4,4) layer of **1**.

Supporting Information



Fig. S2. 1D wave-like [Co-TBTA-Co]_n chain of **2**.

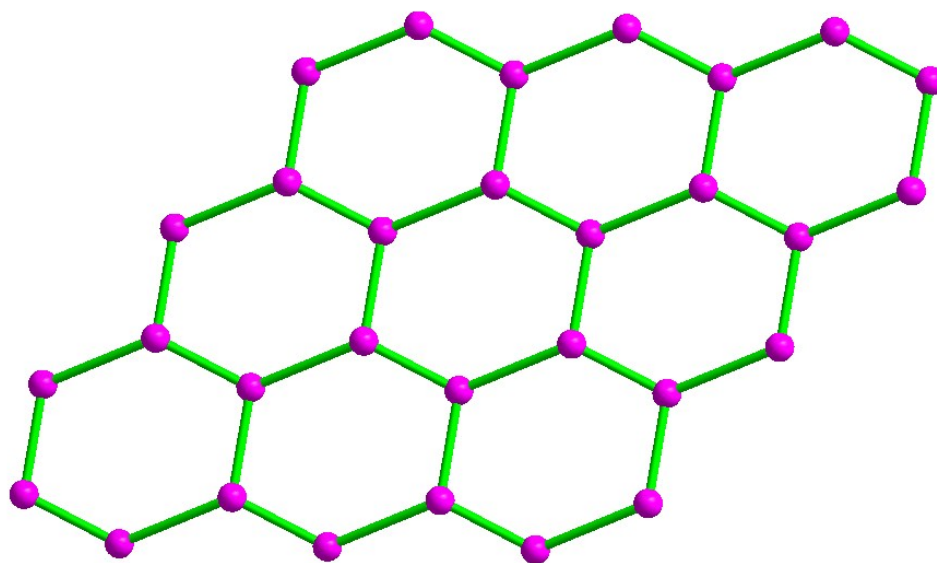


Fig. S3. Uninodal **hcb** topology of **2**.

Supporting Information

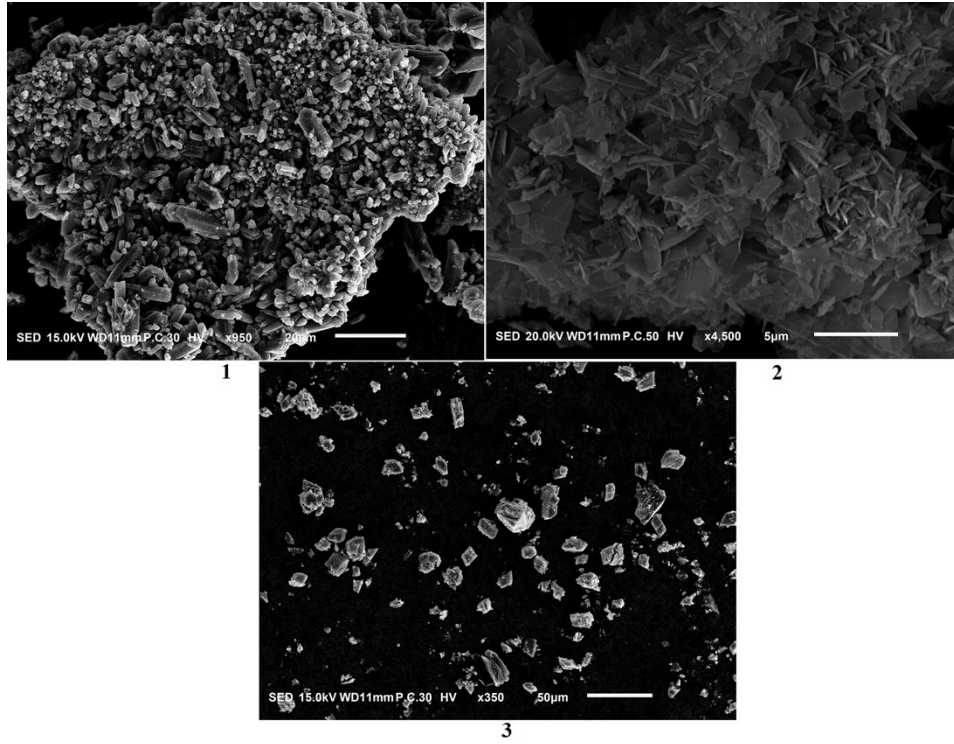


Fig. S4. SEM images of the powdered 1, 2 and 3.

Supporting Information

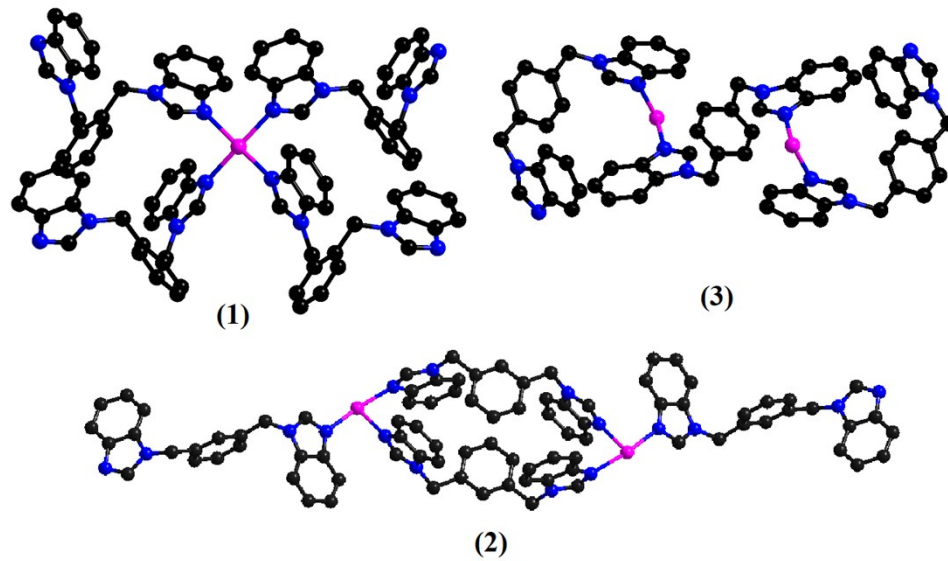


Fig. S5. Different N-containing ligands connect adjacent Co^{II} centers of **1**, **2** and **3**.

Supporting Information

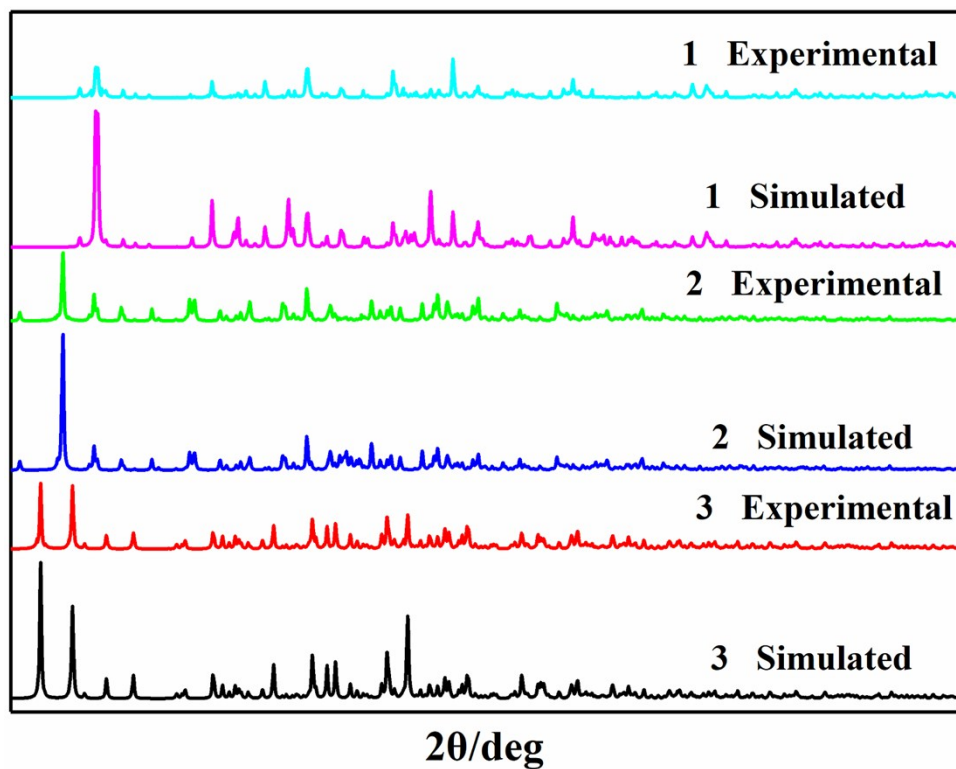


Fig. S6. Powder X-ray diffraction (PXRD) patterns of 1, 2 and 3.

Supporting Information

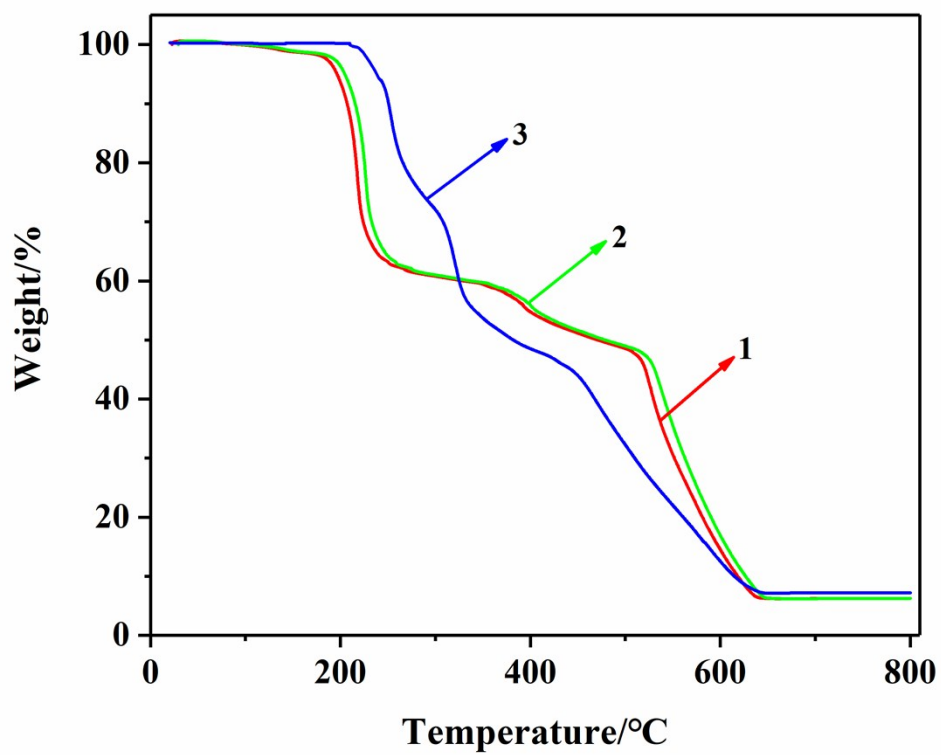


Fig. S7. TGA curves of 1, 2 and 3.

Supporting Information

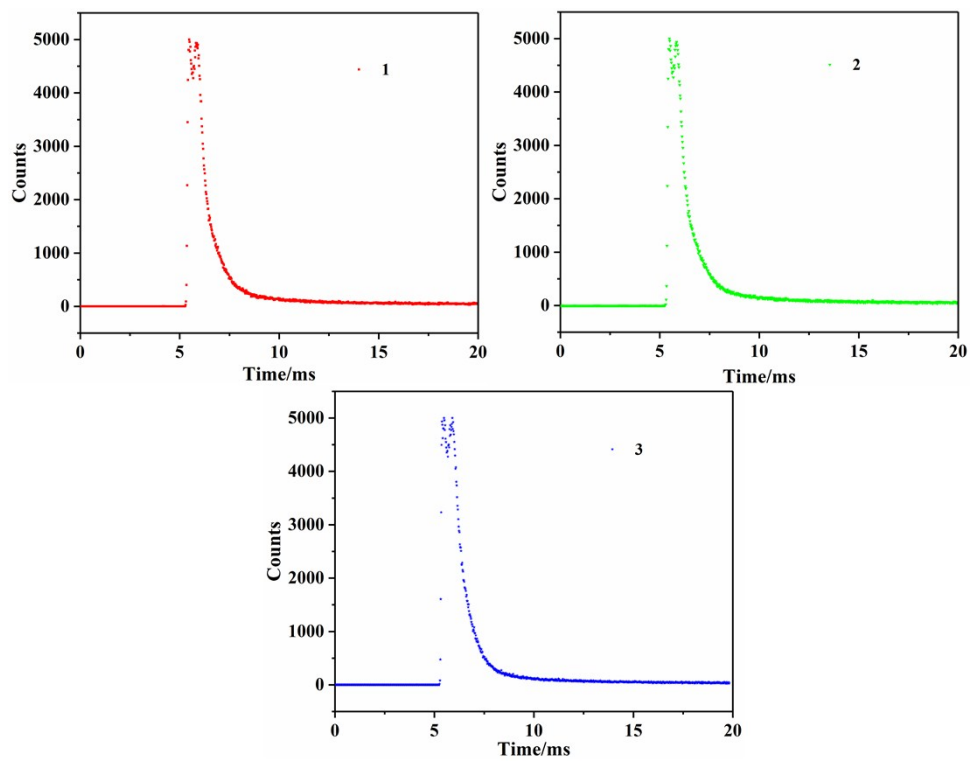
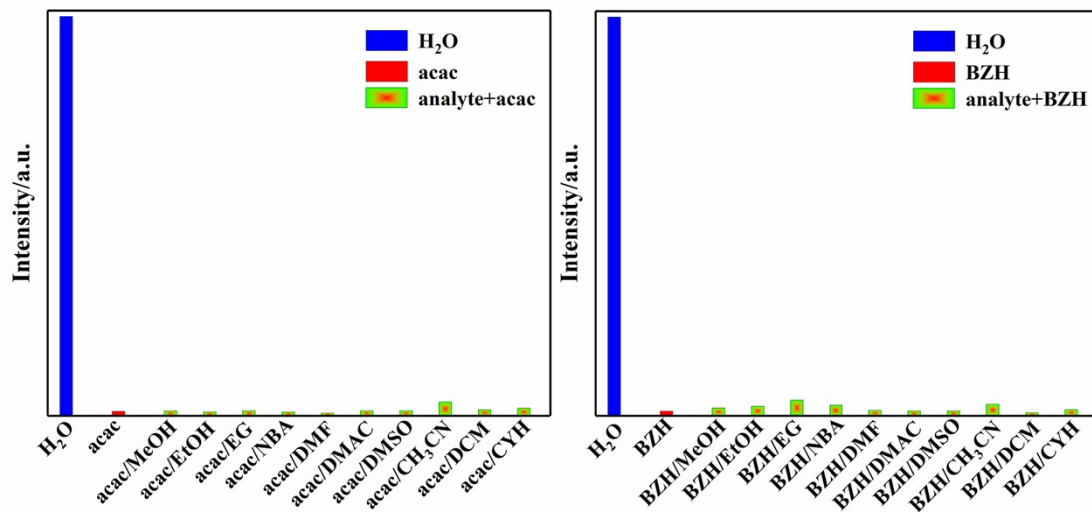
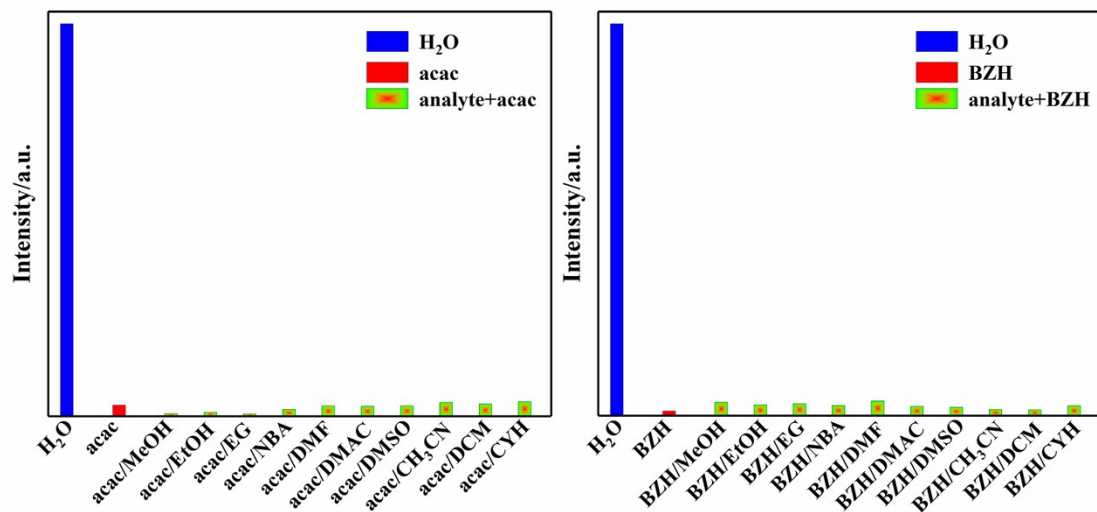


Fig. S8. Time resolved luminescence decay curves of **1**, **2** and **3**.

Supporting Information

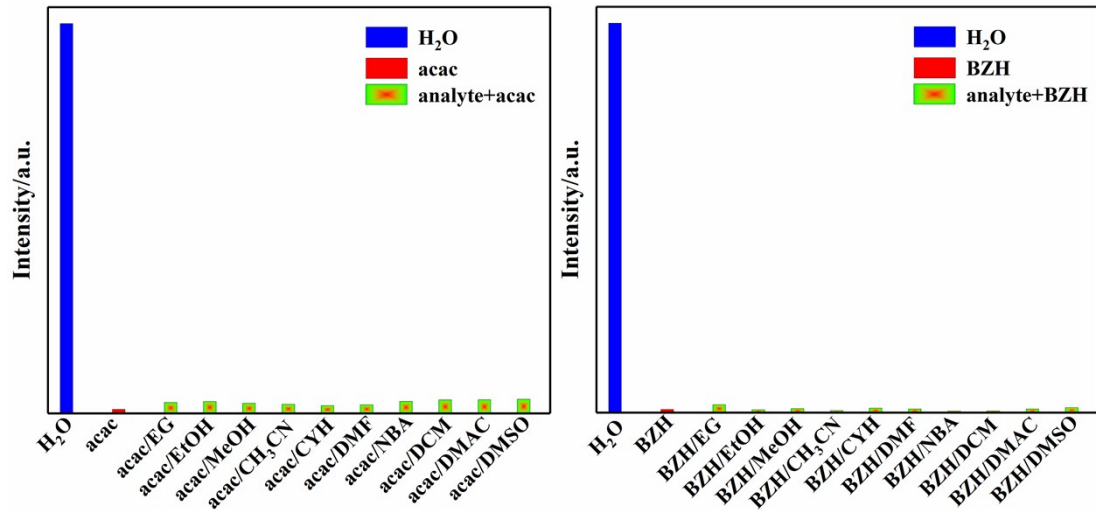


(a)



(b)

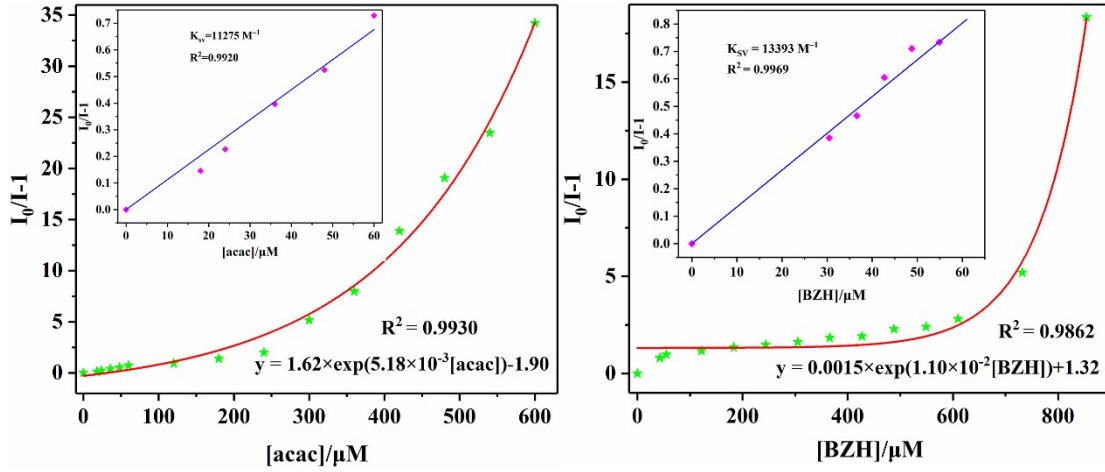
Supporting Information



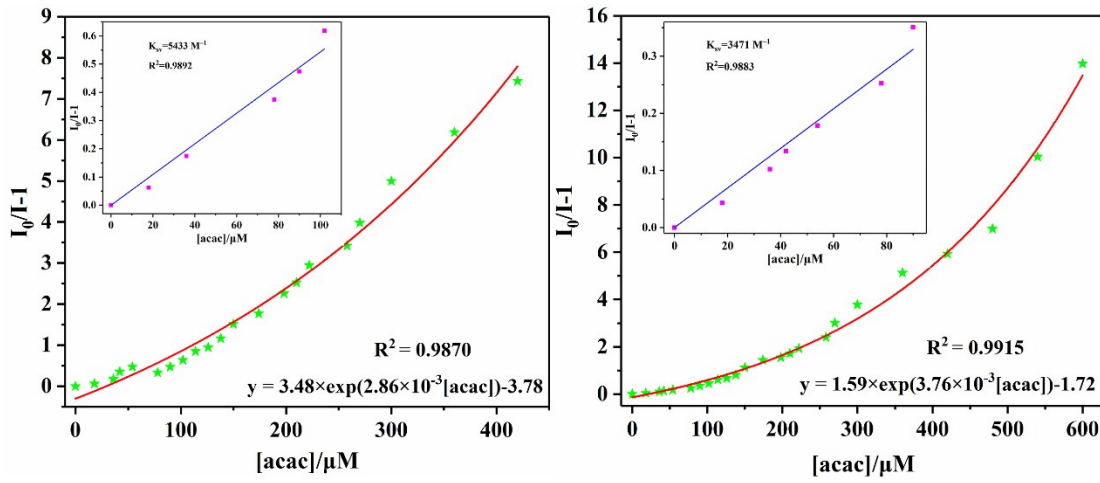
(c)

Fig. S9. (a) Comparison of the luminescence emission intensity of **1** for sensing of acac/BZH in the presence of other organic solvents; (b) Comparison of the luminescence emission intensity of **2** for sensing of acac/BZH in the presence of other organic solvents; (c) Comparison of the luminescence emission intensity of **3** for sensing of acac/BZH in the presence of other organic solvents.

Supporting Information



(a)



(b)

Fig. S10. (a) Stern–Volmer plot of $I_0/I-1$ versus $acac/BZH$ in different concentrations for **2**; (b) Stern–Volmer plot of $I_0/I-1$ versus $acac/BZH$ in different concentrations for **3**.

Supporting Information

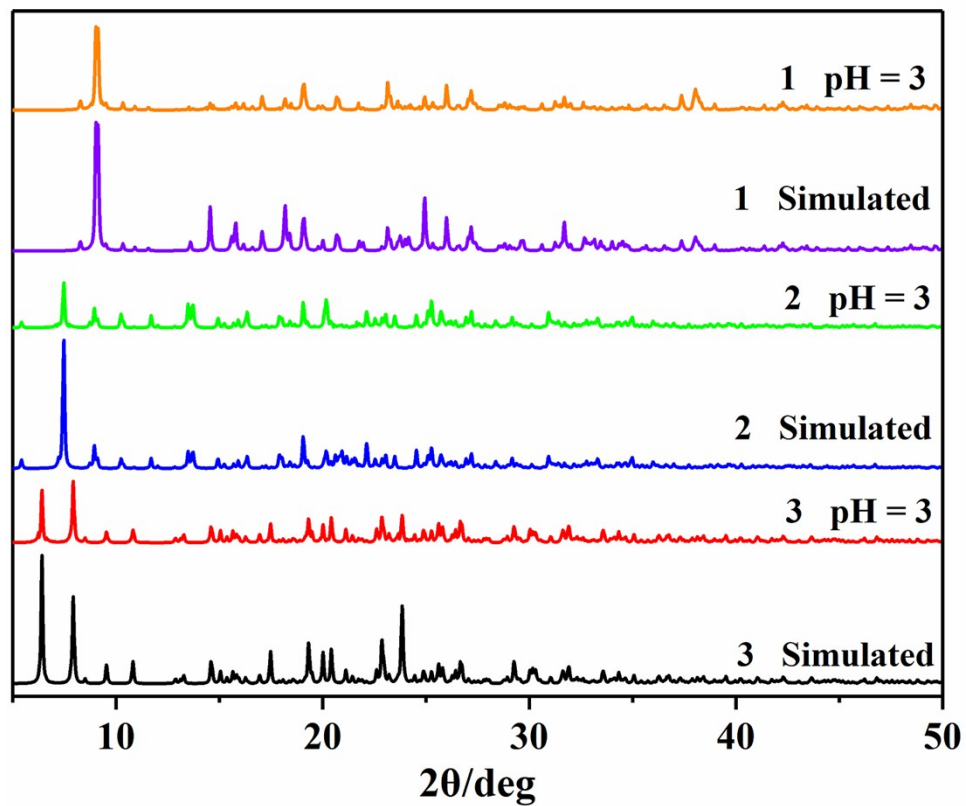


Fig. S11. PXRD patterns of **1**, **2** and **3** after treating in acidic aqueous solution (pH = 3).

Supporting Information

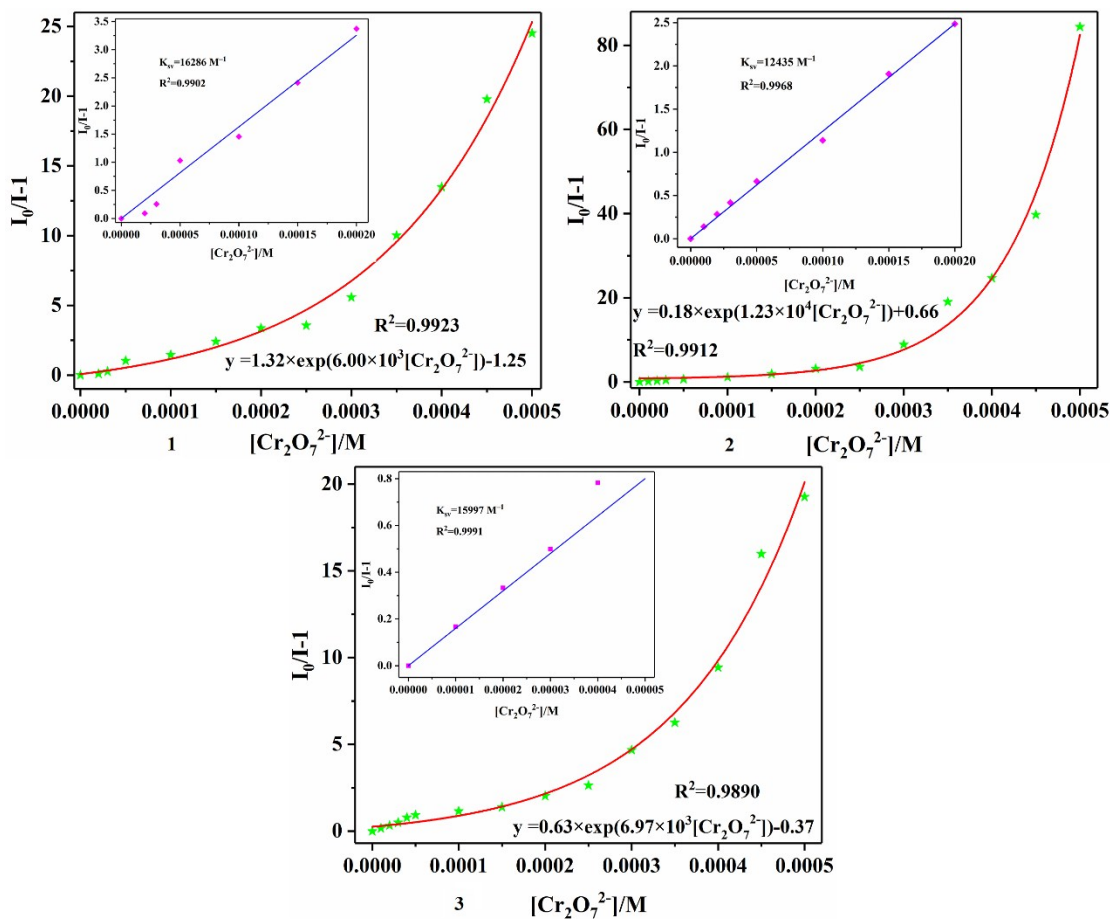


Fig. S12. Stern–Volmer plot of $I_0/I-1$ versus $\text{Cr}_2\text{O}_7^{2-}$ ions in range from 0 to 2×10^{-4} M (top); Nonlinear Stern–Volmer of **1**, **2** and **3** in aqueous solutions with different concentrations (bottom).

Supporting Information

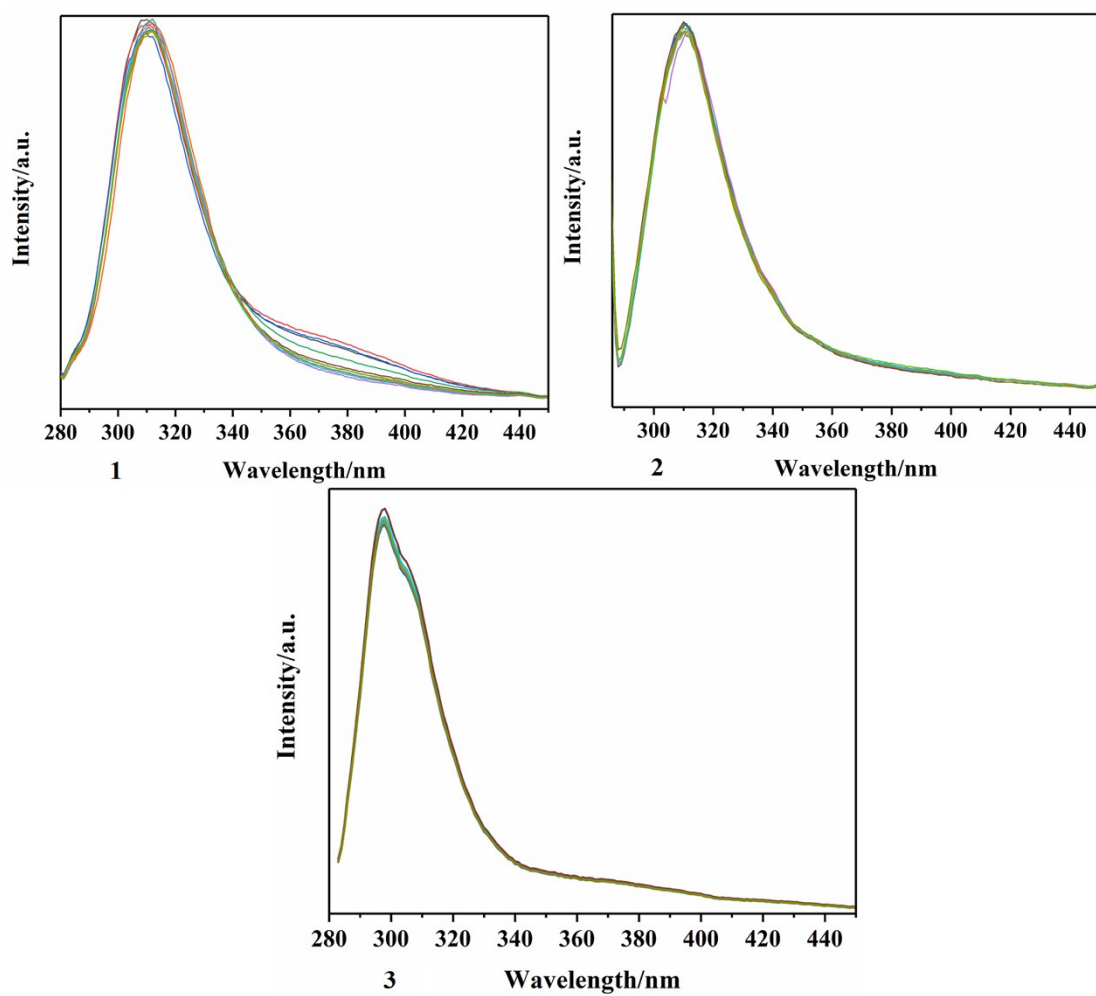
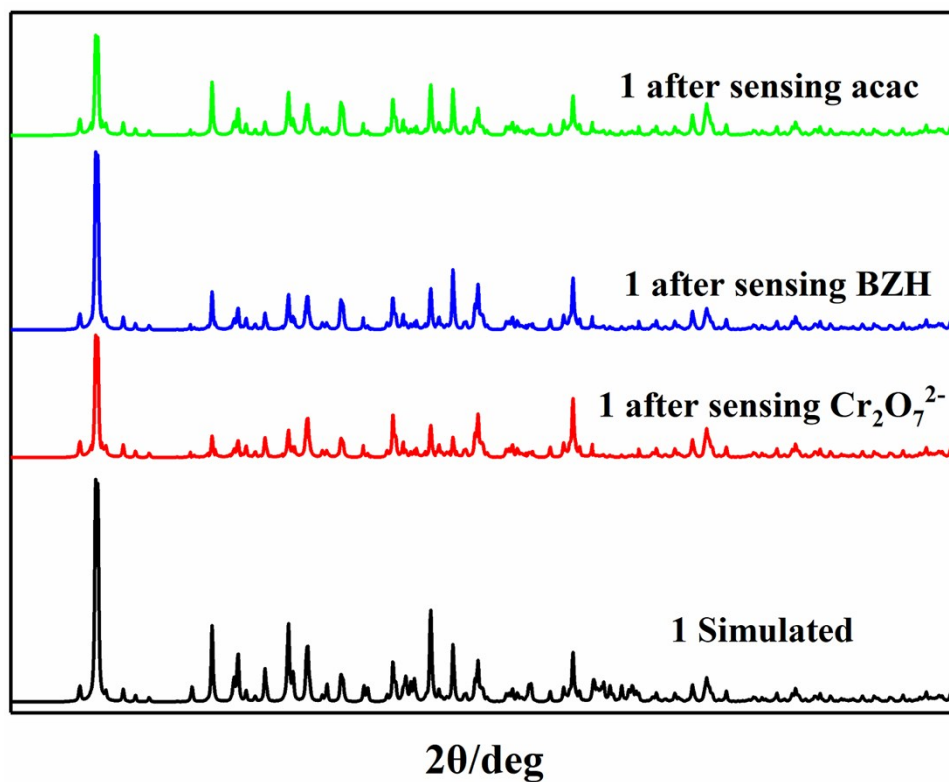


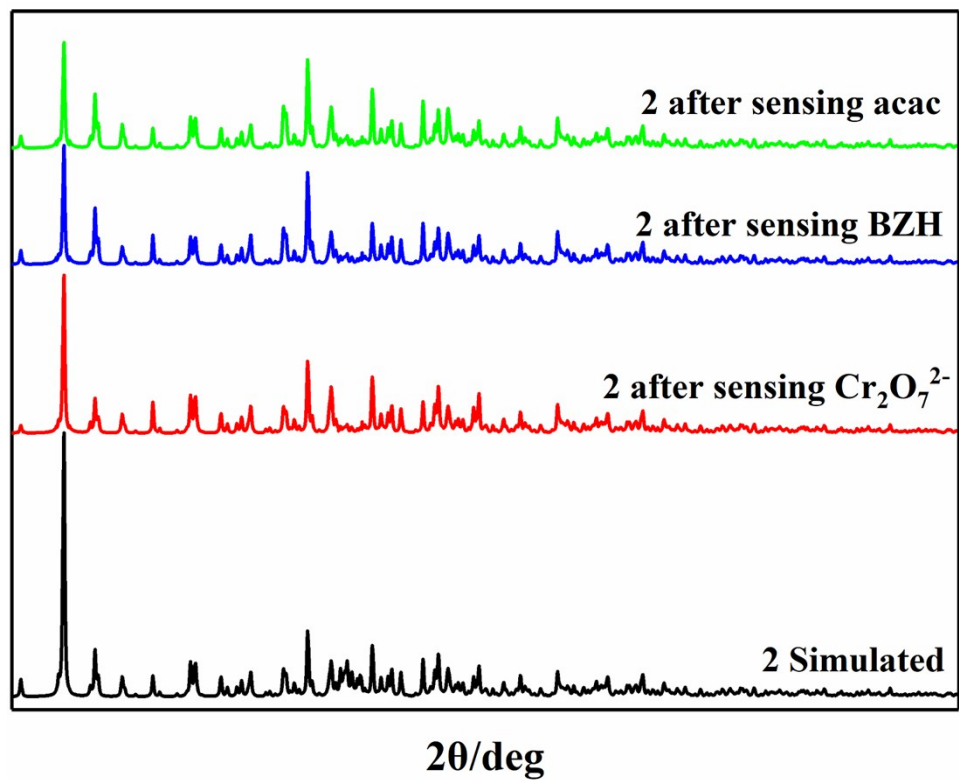
Fig. S13. Luminescence emission spectra of **1**, **2** and **3** in water from 0 to 60 min by 5 min step.

Supporting Information



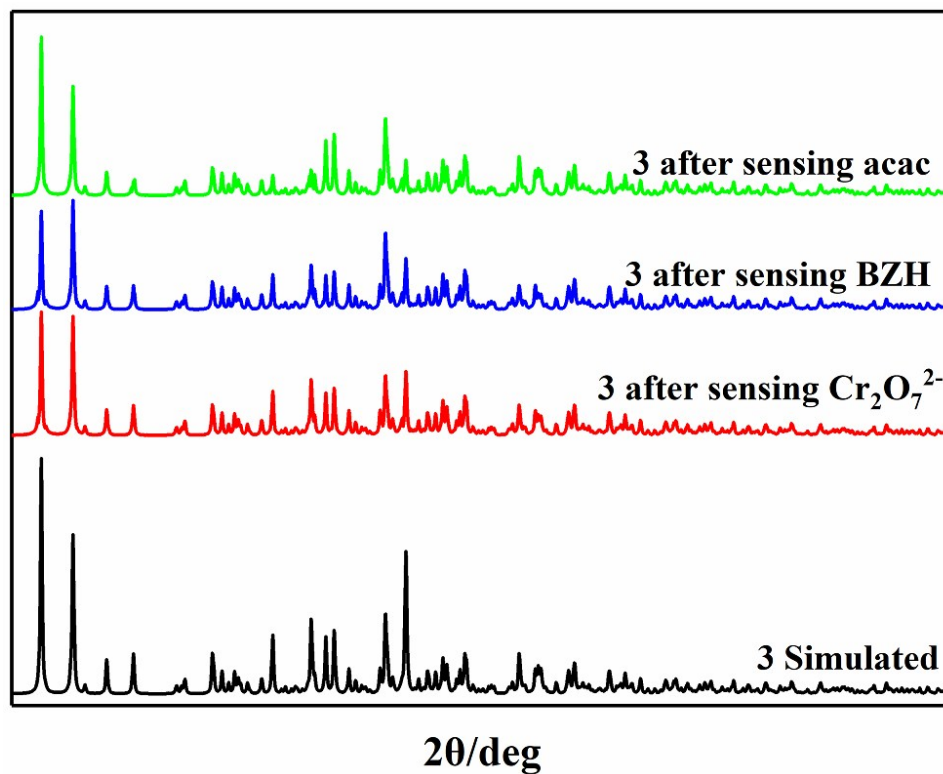
(a)

Supporting Information



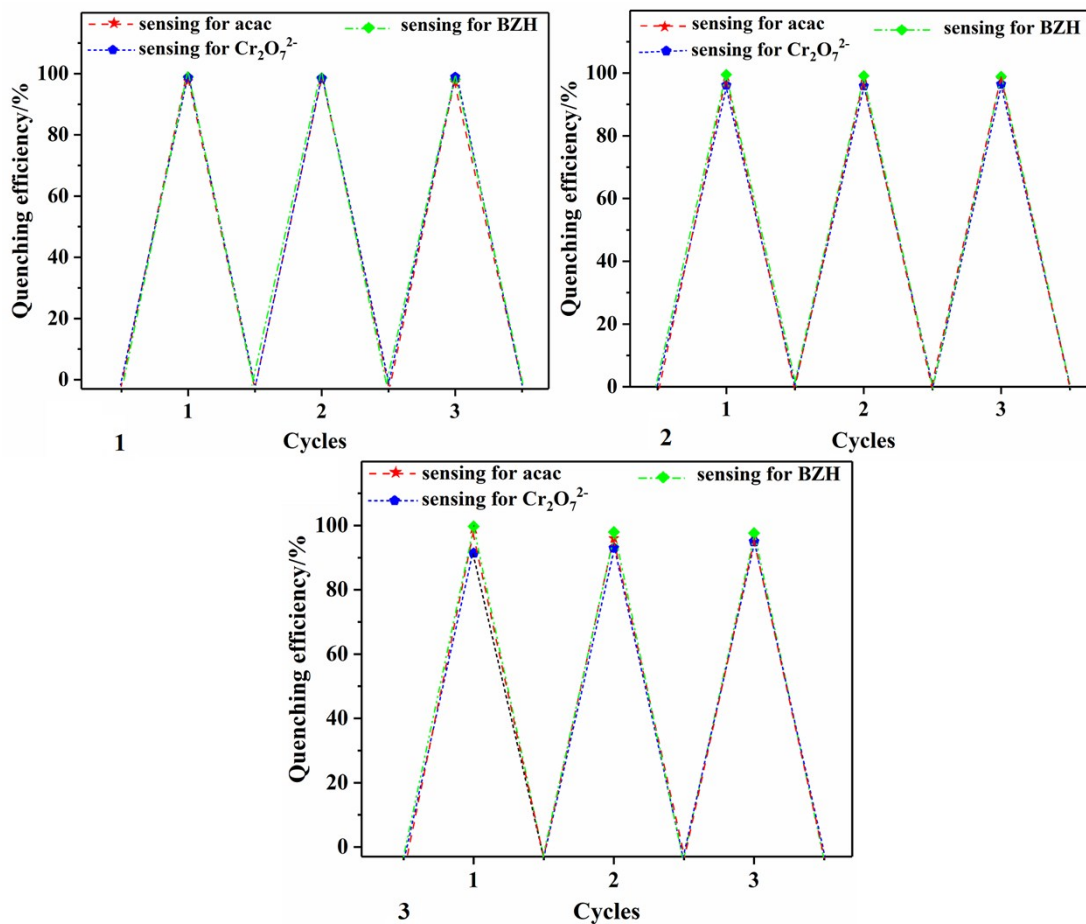
(b)

Supporting Information



(c)

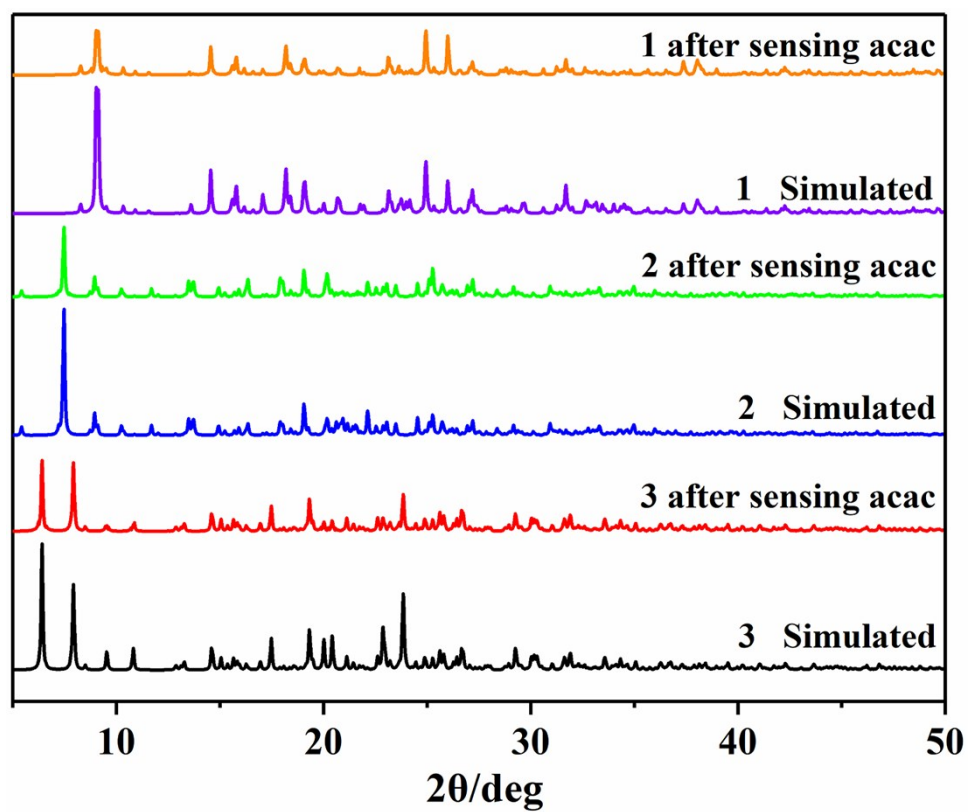
Supporting Information



(d)

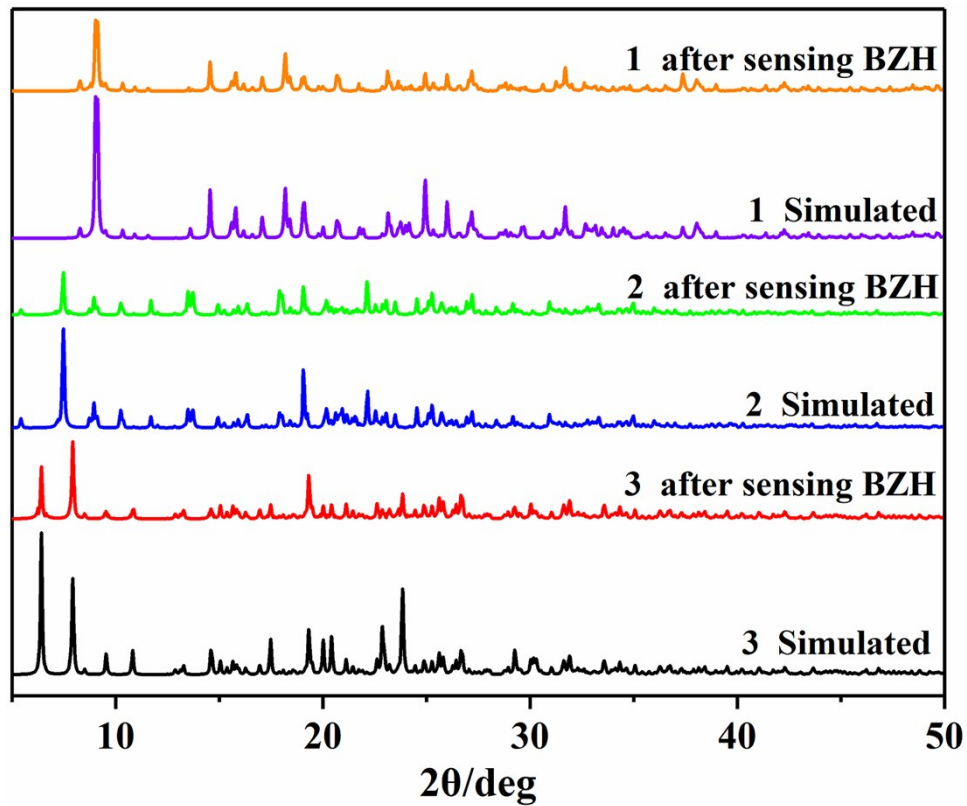
Fig. S14. (a) PXRD patterns of the simulated of **1** after sensing of acac, BZH and $\text{Cr}_2\text{O}_7^{2-}$ for three cycles in water; (b) PXRD patterns of the simulated of **2** after sensing of acac, BZH and $\text{Cr}_2\text{O}_7^{2-}$ for three cycles in water; (c) PXRD patterns of the simulated of **3** after sensing of acac, BZH and $\text{Cr}_2\text{O}_7^{2-}$ for three cycles in water; (d) Comparison of the quenching efficiency of **1**, **2** and **3** for sensing of acac, BZH and $\text{Cr}_2\text{O}_7^{2-}$ over three cycles.

Supporting Information

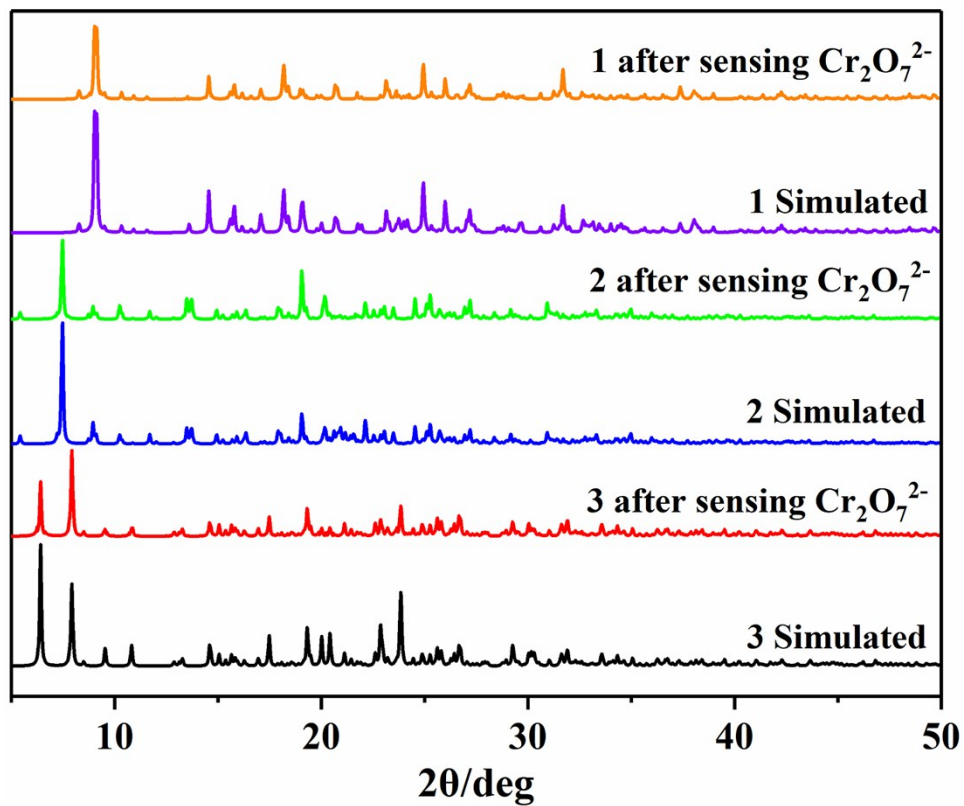


(a)

Supporting Information



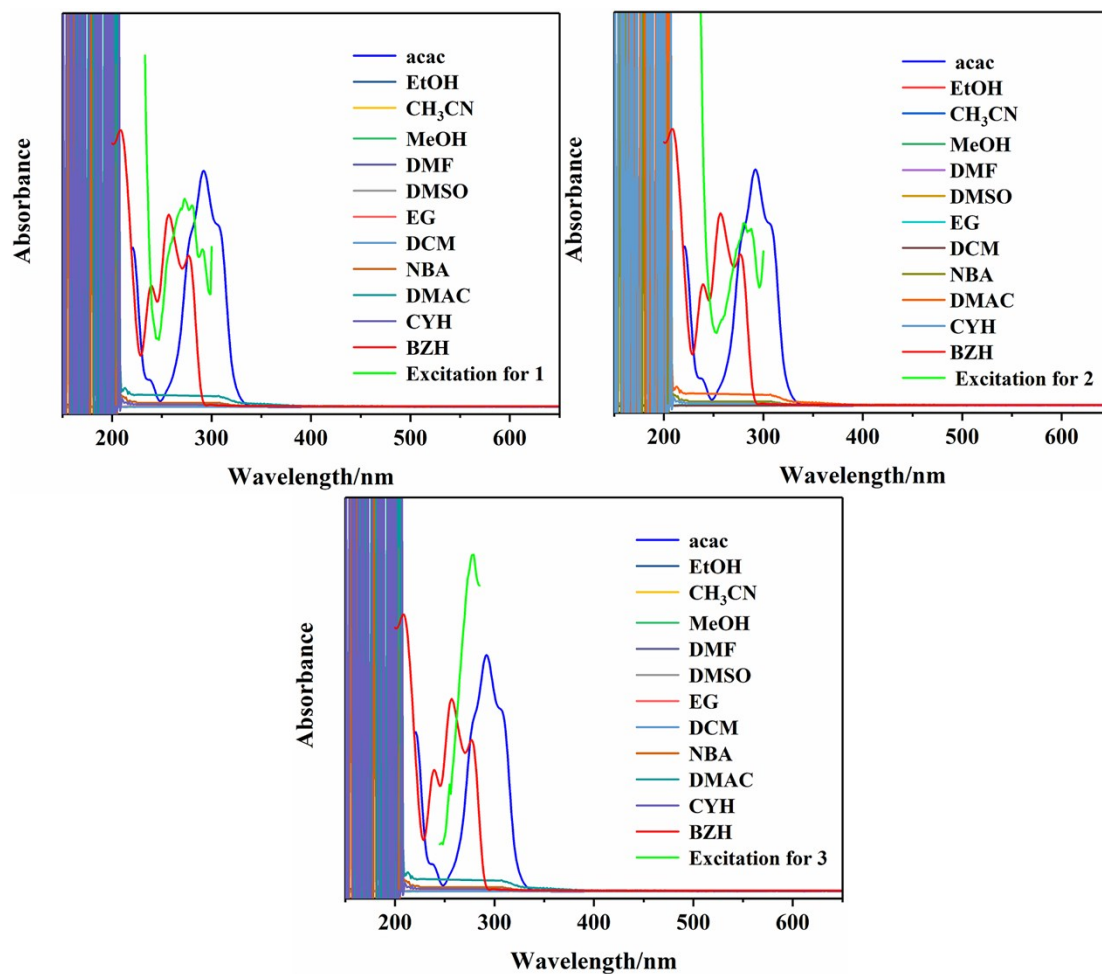
(b)



(c)

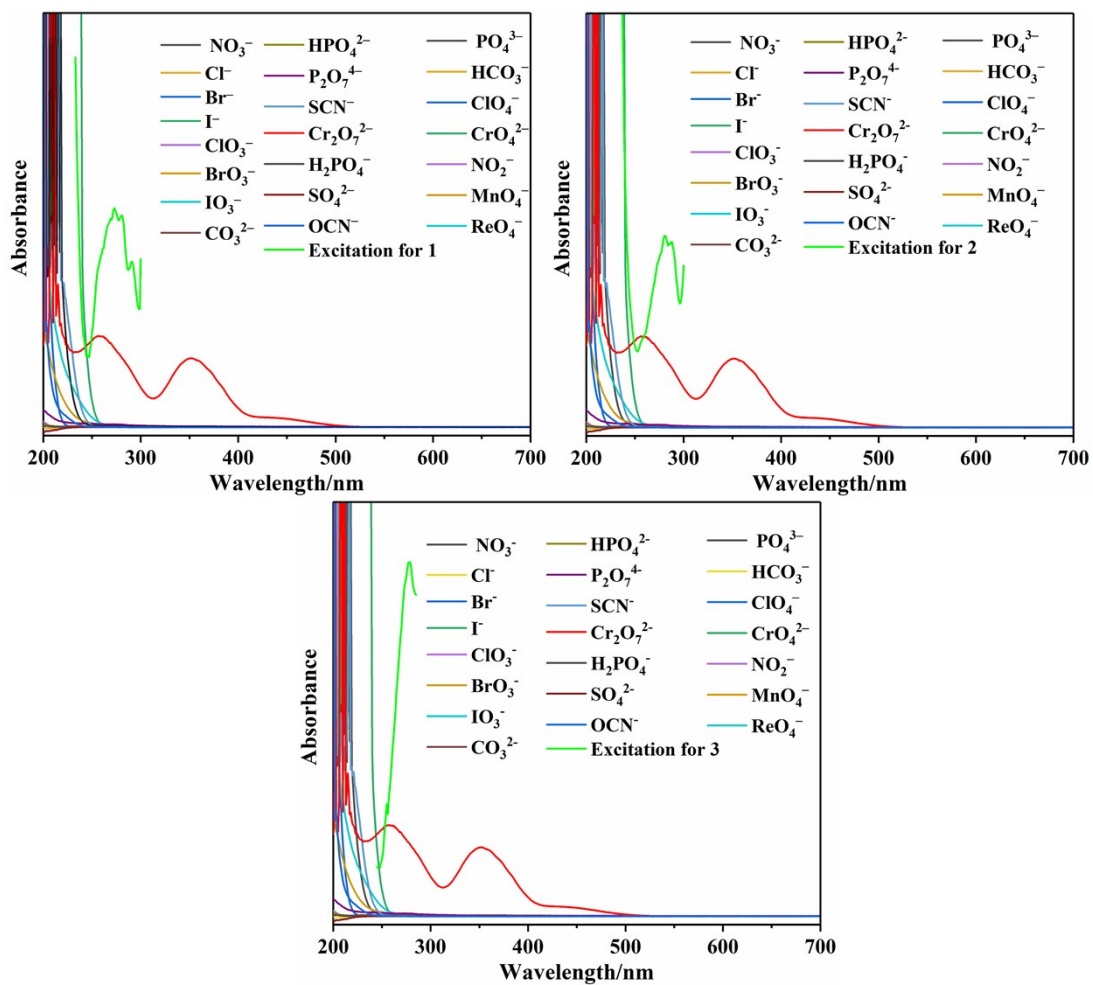
Fig. S15. (a) PXR D patterns of CPs and sensing for acac, respectively; (b) PXR D patterns of CPs and sensing for BZH, respectively; (c) PXR D patterns of CPs and sensing for Cr₂O₇²⁻, respectively.

Supporting Information



(a)

Supporting Information



(b)

Fig. S16. (a) Spectral overlap between the absorption spectra of different solvents and the excitation spectra of **1**, **2** and **3**; (b) Spectral overlap between the absorption spectra of anions and the excitation spectra of **1**, **2** and **3**.